ELSEVIER

Nuclear Instruments and Methods in Physics Research A 484 (2002) 1–16

NUCLEAR INSTRUMENTS & METHODS IN PHYSICS RESEARCH Section A

www.elsevier.com/locate/nima

Transverse profile monitor using ion probe beams

J. Bosser[a,*], C. Dimopoulou[b], A. Feschenko[c], R. Maccaferri[a]

[a] *CERN, PS-Division, BD Group, CH-1211 Geneva 23, Switzerland*

[b] *Institute of High Energy Physics, Lausanne University, CH-1015 Lausanne, Switzerland*

[c] *Institute for Nuclear Research, Russian Academy of Sciences, 60th October Anniversary Prospekt 7A, RU-117 312 Moscow, Russia*

Received 18 January 2001; received in revised form 13 August 2001; accepted 14 August 2001

Abstract

A profile monitor is described that makes use of a low-intensity and low-energy ion beam to measure the transverse profile of a dense proton beam of small dimensions. Three techniques are considered based on the use of ion beams having a pencil, curtain, or cylindrical shape. The detector is almost non-interceptive for the proton beam and does not introduce disturbances in the machine environment. The theoretical aspects of the techniques used, together with experimental results obtained at the CERN SPS and Linac, are presented. © 2001 Elsevier Science B.V. All rights reserved.

PACS: 29; 29.25

Keywords: Profile; Monitor; Ion beam; SPS; Linac; Curtain; LHC; Beam instrumentation; Resistive plate; CCD camera

1. Introduction

The aim of this detector is to measure the transverse distribution of small-dimension, high-density particle beams. The principle on which the detector is based has been reported in Refs. [1–3]. It relies on the deflection of a low-energy, pencil beam of ions passing perpendicularly through a dense particle beam. In the present paper, the analysed (or probed) beam consists of protons. The proof of principle was reported in Ref. [4] (An exhaustive list of relevant papers is given in this reference), after experiments made on the CERN Super Proton Synchrotron (SPS) beam, and in Ref. [5].

In addition to the pencil-beam technique, two further methods are also considered. They are based on the use of an 'ion curtain' [4,6] and on the 'shadowing' effect induced by the analysed beam [4,7] on a cylindrical probe beam.

All three methods are practically non-interceptive and do not perturb the machine environment, in particular the vacuum.

After a brief description of the principles, a summary of the set-up and of the measurements made at the CERN SPS will be given. Though it was initially intended to measure Large Hadron Collider (LHC)-type beams, we shall also mention the possible use of such an ion 'profilometer' on other machines.

*Corresponding author. Tel.: +41-22-767-3786; fax: +41-22-767-9145.

E-mail address: jacques.bosser@cern.ch (J. Bosser).

PII: S0168-9002(01)01965-9

2. Principle

A low-energy ($E_k = 2$–5 keV) ion beam is generated at: ($x = -x_i,\ y = y_0 \ll |x_i|,\ z = 0$) and moves with initial velocity $\vec{v}_i = v_0\vec{e}_x$ perpendicular to the direction of the proton beam. The proton beam itself, centred at (0,0,0) moves with velocity $\vec{v}_{proton} = v_{proton}\vec{e}_z$ (Fig. 1).

The proton beam is supposed to be very dense and has a transverse distribution function with r.m.s. values σ_x and σ_y and a uniform longitudinal distribution over L_b. For simplicity, we suppose a

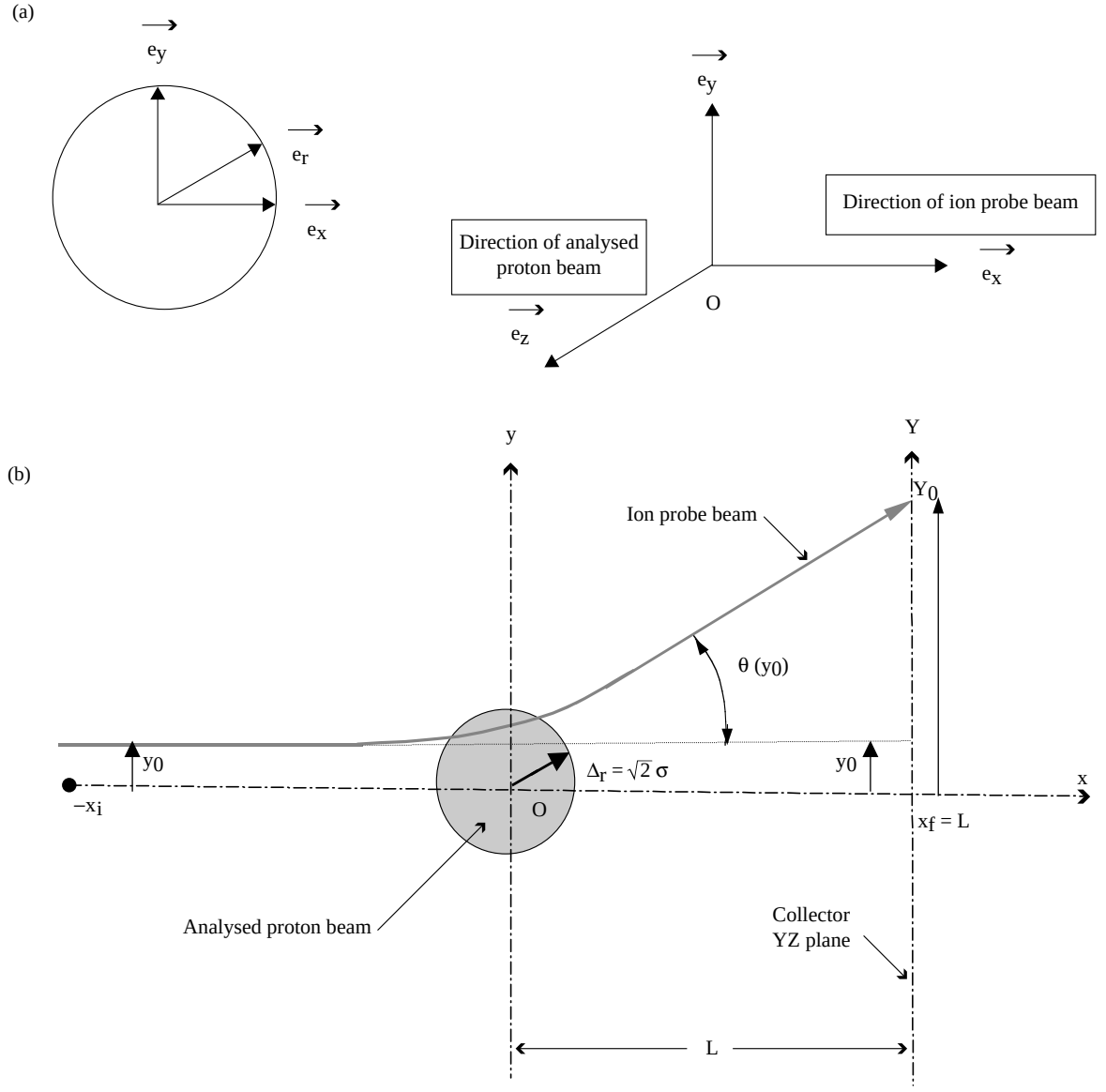

Fig. 1. (a) System of coordinates. (b) Principle of the ion pencil-beam 'profilometer'.

round Gaussian beam ($\sigma_x = \sigma_y = \sigma$, $\Delta_r = \sqrt{2}\sigma$) so that the normalized transverse distribution is given by

$$n_\perp(r) = \frac{2}{2\pi\Delta_r^2}\exp\left(-\frac{r^2}{\Delta_r^2}\right), \quad r = (x^2+y^2)^{1/2}. \quad (1a)$$

The restriction to a round Gaussian beam is not essential; in Refs. [4,5] it is clearly demonstrated that the statements hereafter still remain valid for other realistic proton distributions. This has also been shown in earlier papers (Refs. [2,3]).

The protons are supposed to be relativistic ($v_{\text{proton}} \cong c$) so that the electric space-charge field of the proton bunch is mainly radial $\vec{E}_r = E_r\vec{e}_r$. Gauss's law gives

$$E_r = \frac{V_0}{r}\left[1 - \exp\left(-\frac{r^2}{\Delta_r^2}\right)\right] \quad (1b)$$

with

$$V_0 \equiv \frac{e}{4\pi\varepsilon_0}\frac{2n_b}{L_b}$$

where n_b is the number of protons per bunch and L_b the bunch length. The relativistic condition is not absolutely necessary (see Refs. [4,5]) but will be considered as being fulfilled in this paper except where mentioned.

The ion with charge Q is deflected in the electric field $\vec{E}_r$. For each 'impact parameter' y_0 the ion collector in the YZ plane records the position Y_0 of the ion beam. The position y_0 is recorded when the proton beam is OFF. Then the deflection angle $\theta(y_0)$ can be obtained by

$$\text{tg}\,\theta(y_0) \cong \theta(y_0) = \frac{Y_0 - y_0}{L}.$$

In practice, instead of a single ion, one uses an ion pencil beam of small diameter ϕ_i and small intensity I_i. The collector is aimed then to measure the centre of gravity of the impinging pencil beam.

It has been shown ([1–5] and Appendix A) that, in the case of a Gaussian beam, with minor simplifications the deviation angle θ can be expressed by

$$\theta(y_0) = \frac{QV_0}{2E_k}\pi\,\text{erf}\left(\frac{y_0}{\Delta_r}\right) = \theta_{\max}\,\text{erf}\left(\frac{y_0}{\Delta_r}\right) \quad (2a)$$

with

$$\theta_{\max} \equiv \frac{QV_0}{2E_k}\pi \quad (2b)$$

and the error function is defined by

$$\text{erf}(u) \equiv \frac{2}{\sqrt{\pi}}\int_0^u e^{-\xi^2}\,d\xi.$$

A plot of $\theta(y_0)$ is given in Fig. 2.

For a given ion kinetic energy E_k and ion charge, the maximum deviation angle is independent of the ion mass. The angle $\theta_{\max}$ is proportional to the number of protons per bunch n_b.

By differentiation of Eq. (2a)

$$\frac{d\theta(y_0)}{dy_0} = \frac{2\theta_{\max}}{\sqrt{\pi}\Delta_r}\exp\left(-\frac{y_0^2}{\Delta_r^2}\right) \quad (2c)$$

and so the proton beam transverse r.m.s. dimension is evaluated (Fig. 2).

$$\Delta_r = \frac{2\theta_{\max}}{\sqrt{\pi}}\frac{1}{d\theta/dy_0|_{y_0\cong 0}}. \quad (2d)$$

Eq. (2c) is equivalent to Eq. (1) and therefore represents the distribution that we intend to retrieve from our measurements.

One can observe that $\theta(y_0)$ is linear around $y_0 = 0$ and that $\theta(|y_0| \geqslant \Delta_r) \cong \theta_{\max}$. This asymptotic behaviour is an important characteristic of the detector since it implies that the deflection angle reaches its maximum when the impact parameter is about equal to the proton-beam transverse r.m.s. dimension Δ_r.

Having measured $\theta(y_0) = (Y_0 - y_0)/L$, where y_0 takes its values over a significant interval around the proton beam (at least $-3\Delta_r \leqslant y_0 \leqslant 3\Delta_r$), one can deduce $\theta_{\max}$ and $d\theta(y_0)/dy_0$.

The radial r.m.s. value Δ_r can then be obtained from Eq. (2d). However, in some cases, this method of data treatment might not be very precise because some errors are induced by the numerical derivation of $\theta(y_0)$. It is then employed only for rough estimates, and more elaborate numerical smoothing techniques are needed.

We suppose here that the ion velocity v_0 and the bunch duration $\sigma_t = L_b/c$ are such that the ion

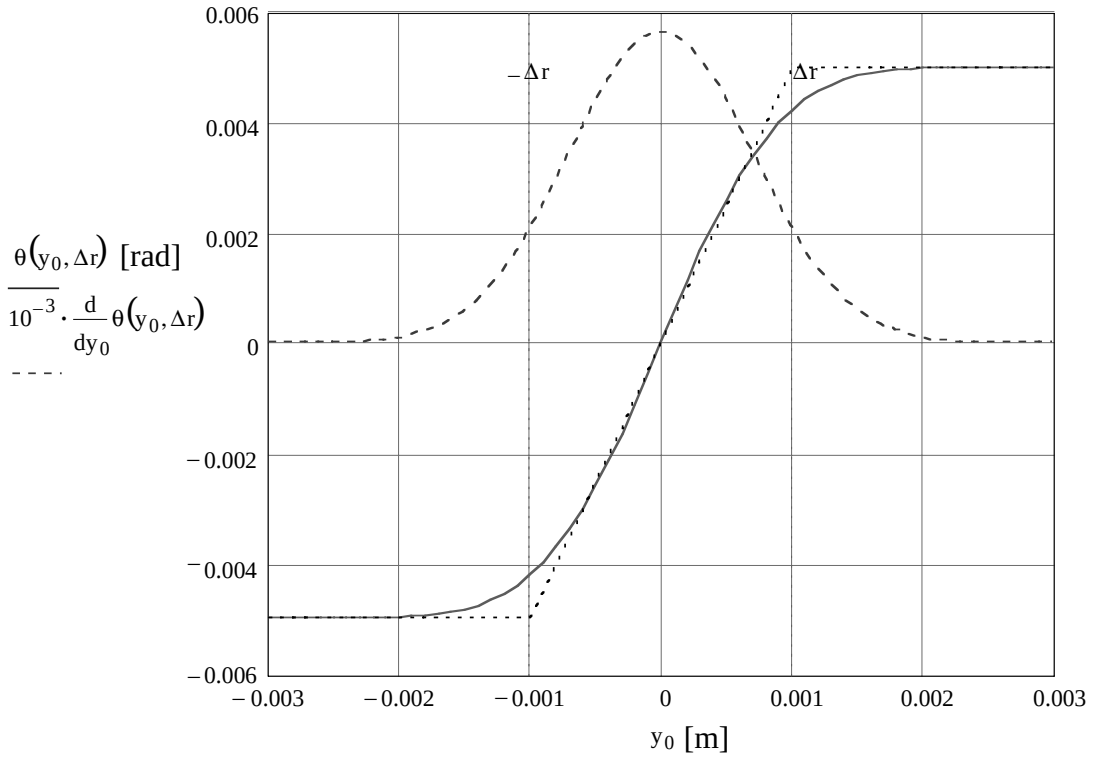

Fig. 2. Plot of the deflection angle [Eq. (2a)] for $\Delta_r = 1$ mm and $\theta_{max} = 5$ mrad (solid curve), the dotted curve is an approximation of the deflection angle by straight lines. A plot of $d\theta(y_0)/dy_0$ multiplied by an arbitrary constant is also given (dashed curve).

interacts only once with the bunch on its way from the gun to the detector.

Since from Eq. (1b) the proton beam electric field is effective in a radius $r \simeq \pm 5\Delta_r$, this condition can be expressed as follows:

$$\frac{10\Delta_r}{v_0} \leqslant \sigma_t. \qquad \text{(condition 1)}$$

For an unbunched proton beam, condition 1 is of course fulfilled. All the formulas above are valid if we replace n_b and L_b in the expression $V_0 \equiv (e/4\pi\varepsilon_0)(2n_b/L_b)$ by the number of circulating protons and the machine circumference, respectively.

In the case where condition 1 is not fulfilled, i.e. $(10\Delta_r/v_0) \gg \sigma_t$, the ion will receive small kicks at each passage of a bunch, of duration σ_t, and will not be subject to any electric force during the time interval between two bunches T. The trajectory is more complicated. A rough approximation can, however, be obtained by simply replacing the parameter V_0 in Eq. (1b) by

$$V_0' \equiv V_0 \frac{\sigma_t}{T}.$$

A modulation of the deflection angle with time occurs [4,5] since the ion will sense no electric field during the time interval between two consecutive bunches. This effect is quite small and even negligible in the present case where we use a heavy probe ion (Ag^+ or Xe^+) moving at relatively small velocity. As complementary information, this monitor will also provide the proton-beam position or centre of gravity y_{cg} where the ion beam is not deflected.

A detailed simulation program has been developed [4,5]. It includes all the proton beam parameters as well as the detector environment (such as the vacuum pipe dimensions, etc.) and is a

good tool for interpreting and analysing our experimental results.

3. The different collector types

The aim of the collector is to measure the impinging ion-beam position (or more precisely its centre of gravity), equal to y_0 when the proton beam is OFF, and to Y_0 when the beam is ON.

The ion current intensity is rather small (a fraction of nA) such that in some cases the use of Micro-Channel Plates (MCPs), which convert the incoming ions into electrons, might become necessary. The MCP gain can be of the order of 10^4.

We have used three different position detectors with and without MCPs:

(a) Equally spaced metallic microstrips. Up to 32 strips, spaced at 1.5 mm, were used. The current collected by each strip is integrated before being processed. The scanning time through the proton beam can be as low as 1 ms.
(b) A resistive plate with adequate time constant. An integrator is placed at each end, A and B, of the plate. The ratio $D/S = (A - B)/(A + B)$ is proportional to the position of the centre of charges (or centre of gravity) of the impinging beam. The overall scanning time can be of the order of 0.1 ms.
(c) A luminescent screen viewed by a CCD camera. The image is processed every 20 (or 40) ms so as to determine the ion-beam position or, as we shall see in Section 8, the ion density distribution. There is also the possibility of sampling the probe beam within a very short time (about 1 μs); but the image processing time can be much longer.

In the case of a stored or stable proton beam averaging and/or filtering is easy. Therefore, in the case of a stored beam, at fixed energy and intensity, one can also foresee to use the monitor as a 'watchdog' continuously measuring the maximum deviation angle; in other words, the variation of the transverse proton beam dimension.

4. Ion source main parameters

The ion source (gun and associated optics) plays an important role; and is an industrial product with significant modifications implemented by us.

The source can provide not only a pencil beam but can also be arranged so as to deliver an ion curtain or a wide cylindrical beam. In this section we shall nevertheless limit our analysis to the pencil-beam source represented by Fig. 3.

It is evident that the source must provide an ion beam (a) as intense as possible in order to obtain

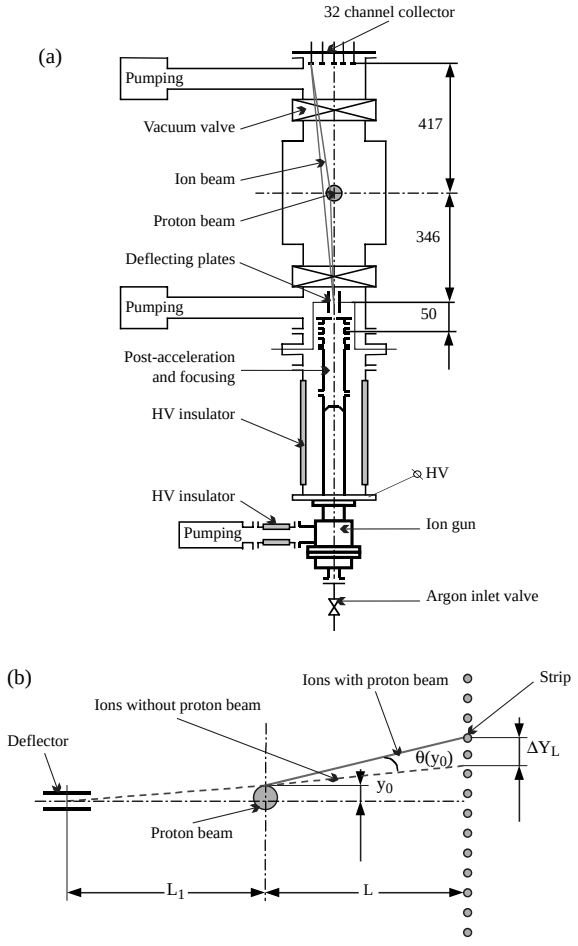

Fig. 3. Ion pencil-beam technique. (a) Experimental set-up as implemented on the SPS machine. All dimensions are in millimetres. (b) Details of 3(a) where it is shown that in the present set-up the ion beam is not perpendicular to the proton beam but has a small incident angle.

good accuracy from the collector; (b) of small diameter ϕ_i, a fraction of Δ_r; and (c) of small divergence, a fraction of θ_{max}.

Measurements showed [4,5] that, 15 mm after the gun output, the emittance of a $E_k = 2$ keV ion beam is 5.5 mm mrad for an ion current $I_i =$ 50 nA (and 4 mm mrad when $E_k = 5$ keV).

After the ion gun (at potential U_s such that $E_k = QU_s$) the ion beam passes through a drift tube. At the drift tube output the ion beam is focused by an 'Einzel lens' and then collimated. The collimator system consists of slits restricting the beam dimension and angle in the plane of interest. At the collimator output the beam is deflected by electrically charged plates so that it crosses the proton beam at an angle. A future version of the ion source foresees a parallel displacement to vary the impact parameter y_0.

We require a beam with diameter $\phi_i = 0.2$ mm and divergence 1.0 mrad in the plane of interest. In such a case the current is reduced down to about 1 nA by the slits acting as collimators. Such a current, collected on one strip of the detector, will result in a voltage of 20 mV when integrated during 1 ms by a 50 pF capacitance. Such a signal can be accurately processed. Lower beam intensities require the use of an MCP as amplifier.

On its way from the source to the collector, at distance $L_x = L_1 + L$, the ion pencil beam of radius $r_i = \phi_i/2$ will naturally expand as a consequence of its own transverse electric field. For a uniformly distributed round ion beam the increase in radius is about

$$\Delta_{r_i} = \frac{Q}{m_i}\frac{1}{4\pi\varepsilon_0}\frac{I_i}{v_0^3}\frac{L_x^2}{r_i} \tag{3}$$

which for argon, $I_i = 1$ nA, $r_i = 0.1$ mm, $E_k =$ 2 keV, $L_x = 1$ m, gives $\Delta_{r_i} = 0.23$ mm, which is just acceptable. In practice Δ_{r_i} is smaller since the ion beam is collimated in one direction only, namely along $\vec{e}_y$ and is rather wide along the $\vec{e}_z$ direction. In the case of such a rectangular-shaped beam of height ϕ_i and width $d_i \cong 1$ cm, r_i must be replaced by d_i in Eq. (3).

The space-charge potential ΔU_s between the centre and the edge of the ion beam will induce a corresponding difference in kinetic energy and therefore different deflection angles. Since for a round beam $\Delta U_s = 30 I_i c/v_0$, the change of deflection angle can be expressed as follows:

$$\left|\frac{\Delta\theta_{max}}{\theta_{max}}\right| = \frac{\Delta E_k}{E_k} = \frac{\Delta U_s}{U_s} = \frac{30 I_i c}{v_0 U_s}.$$

For $U_s = 2$ kV and $I_i = 1$ nA this ratio is very small.

It is evident that higher intensity and lower emittance sources are welcome and under investigation.

5. Choice of the probe particle type

Up to now we have considered heavy ions to be used as probe particles. One might of course consider instead the use of an electron pencil beam whose production is easier. In such a case the effect of the proton-beam azimuthal magnetic field $\vec{B}_\varphi$ (with $|\vec{B}_\varphi| = v_{proton}/c^2|E_r|$) has to be taken into account.

For an ion with velocity v_0 the ratio of the electric force $F_e(r)$ to the magnetic force $F_b(r)$, at a given radius r, is

$$\left|\frac{F_e(r)}{F_b(r)}\right| = \frac{c^2}{v_{proton}\ v_0}. \tag{4}$$

Considering the same maximum deviation angle θ_{max}, for both ion and electron beams, the electron velocity will be $v_e = v_0(Am_p/m_e)^{1/2} \gg v_0$ where A is the ion atomic mass number and so

$$\left|\frac{F_e(r)}{F_b(r)}\right|_{electrons} \leqslant \frac{1}{44\sqrt{A}}\left|\frac{F_e(r)}{F_b(r)}\right|_{ion}.$$

Compared with those of ions, the electron trajectories are significantly influenced by the proton-beam self-magnetic field. Furthermore, leak fields from nearby magnets in the machine will perturb the electron beam. In other words, the electron global trajectory is not straightforward and the measurement of $\theta(y_0)$ is rather difficult. Examples are given in Refs. [4,5].

In addition, the deflection angle modulation, resulting from the ratio $\sigma_t/T < 1$ will be enhanced due to the higher velocity of the electron. Indeed the electron will move over a longer distance between two bunches where it is subject to no transverse electric field.

This is why a heavy-ion source (up to xenon) has been used instead of an electron gun.

6. Profile measurement using an ion pencil-beam

6.1. Principle

The collector consists of 32 strips of 1 mm width, spaced at 1.5 mm. The detector can be isolated completely from the machine by two vacuum valves. Vacuum pumps ensure that practically no pressure increment is recorded on the machine.

6.2. Measurements made on the SPS machine

The ion beam had a diameter of $\phi_i = 0.2$ mm and an intensity of a few nA. The beam was displaced by changing the voltage on the deflection plates.

It must be noticed that in order to simplify the hardware, the ion beam does not cross the proton beam perpendicularly but at an angle $\mathrm{tg}\alpha(y_0) \simeq \alpha(y_0) = y_0/L_1$; in our case $\alpha(y_0)$ is very small since L_1 is much larger than the analysed beam size (Fig. 3b).

The deflection angle is obtained by

$$\theta(y_0) = \frac{Y_0 - y_0}{L} - \frac{y_0}{L_1} \tag{5}$$

where y_0 is measured when the proton beam is OFF. Measurements were made in the horizontal plane.

A first measurement aimed to prove the validity of the principle. The impact parameter y_0 is scanned every SPS cycle and the pencil-beam signal is integrated over 1 s. The measurement of the deflection angle θ as a function of y_0 is given by Fig. 4a. The maximum deflection angle $\theta_{max} \cong 12.5$ mrad is about that expected from Eq. (2b) (in the present case: $n_b = 9 \times 10^9$). Considering some fluctuation in the r.m.s. transverse dimension and in the position from cycle to cycle, the results are plausible.

A second, more global measurement was intended to measure the r.m.s. size at different instants during the SPS acceleration cycle. The integration time was 200 ms. The r.m.s. size Δ_r was obtained by differentiating the angle of deviation $\theta(y_0)$. At the same instants, we measured the proton-beam profile with a wire scanner, and its position with a standard pick-up. Three sets of measurements were made. The comparative results are shown in Fig. 4b.

The r.m.s. beam size measured with the ion pencil-beam appears to be larger than that obtained with the wire scanner. As far as the proton beam position is concerned, there is a good agreement between the measurements obtained with the ion pencil-beam and those made with the SPS pick-up. Anyway, we consider these preliminary experimental results to be promising.

A detailed description of the detector and of the measurements on the CERN SPS machine are given in Refs. [4,8].

7. Profile measurement using an ion curtain

Instead of scanning the ion beam in the y direction, we use a flat ion curtain beam, inclined by an angle φ. For this purpose the ion source has been modified. The principle becomes as described in Fig. 5a.

Without proton beam the thin ion beam is distributed along the line 0ξ of equation $y = Y = z\ \mathrm{tg}\ (\varphi)$ and moves perpendicular to the sheet. With proton beam, each individual ion at ordinate y is deviated by angle $\theta(y)$ and reaches the collector at ordinate $Y = y + L\ \mathrm{tg}\ \theta(y) \cong y + L\theta(y)$.

After some linear transformations we retrieve the distribution $\theta(y)$ and its derivative in a similar way to that explained in Section 2.

A complete description of this type of monitor and of the measurements is given in Ref. [6].

In the present case we used an MCP followed by a luminescent screen [see Section 3(c)]. An example of the observed 'curved' curtain beam is shown in Fig. 5b.

Measurements during the SPS cycle have been made and compared to those, made at the same instants, with the wire-scanner. Results are shown in Fig. 5c and demonstrate a good agreement between the measurements. The corresponding proton-beam distributions are given in Fig. 5d. The accuracy is limited by the image treatment [7], more precisely by the limited number of pixels of the camera. The actual image processing also

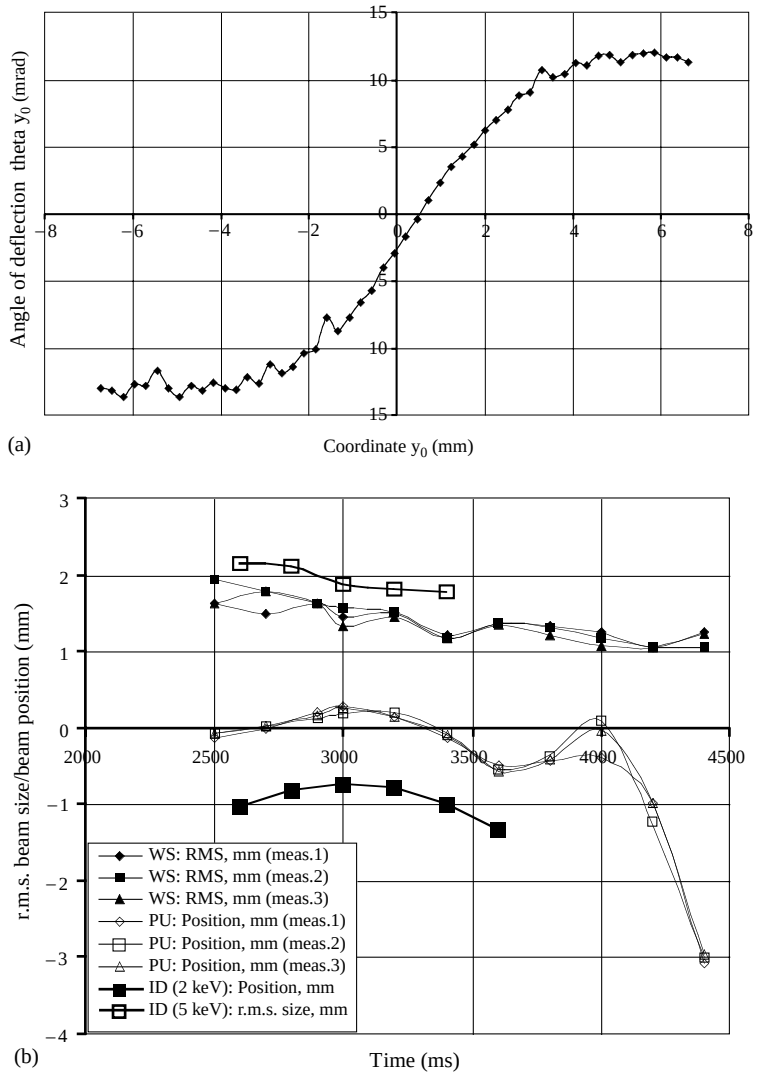

Fig. 4. Measurements made on the SPS in the horizontal plane, using the ion pencil-beam method. (a) Rough measurement of the deflection angle $\theta(y_0)$. (b) r.m.s. size (upper 4 curves) and position (lower 4 curves) measured along the SPS acceleration ramp with the ion profilometer (ID), the wire scanner (WS), and the beam-position pick-up (PU).

limits to 20 ms the time interval between two profile measurements.

8. The shadowing technique

In the shadowing technique [7] (but also mentioned in Refs. [3,4]), we transform the ion source into an almost cylindrical beam. For simplicity, let us consider a cylindrical ion beam with a radius of a few Δ_r moving parallel to the $(-x_i, x_f)$-axis.

The detector is based on the changes in ion density n_i along the $\vec{e}_y$-axis.

When the proton beam is OFF the probe ions lie on the OY line of the observer plane (Fig. 1b) with density $dn_i/dY = dn_i/dy$; dn_i/dy being determined by the ion source properties.

When the proton beam is ON, since $Y = y + L\theta(y) \equiv g(y)$, a measurement of the ion

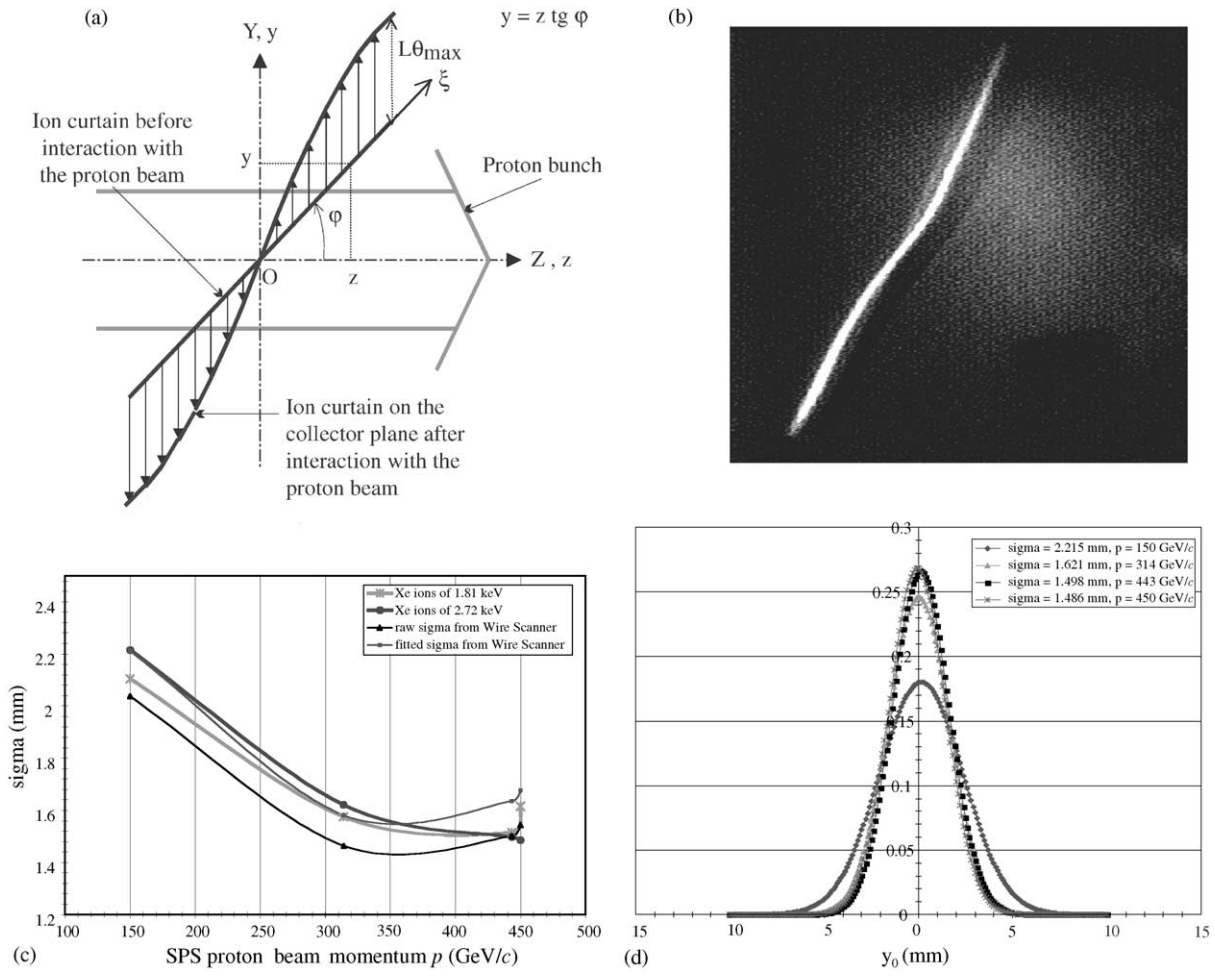

Fig. 5. Ion curtain technique, its use on the SPS machine. The total number of circulating protons was 1.8×10^{13}. We used Xe^{+} ions at 2.72 keV. (a) Principle of the ion curtain profilometer. (b) Image observed on a TV screen showing the 'curved' ion curtain for a 314 GeV/c proton beam. (c) Evolution of proton-beam horizontal r.m.s. dimension (sigma) as a function of its momentum. For comparison, we used a wire scanner located close to the profilometer. Two ion energies are used. (d) Normalized horizontal profiles at some discrete momenta. The corresponding horizontal r.m.s. dimension (sigma) is also given.

density gives

$$\frac{\mathrm{d}n_{\mathrm{i}}}{\mathrm{d}Y} = \frac{\mathrm{d}n_{\mathrm{i}}}{\mathrm{d}y}\frac{\mathrm{d}y}{\mathrm{d}Y} = \left(\frac{\mathrm{d}n_{\mathrm{i}}}{\mathrm{d}y}\right)\frac{\mathrm{d}(g^{-1}(Y))}{\mathrm{d}Y}.$$

A depletion of the ion density as a function of the proton bunch distribution is expected. Fig. 6a illustrates this effect. More details on the interpretation of the measurements are given in Appendix B.

Instead of a cylindrical beam, one could of course consider the ion curtain with $\varphi = \pi/2$ (see Fig. 5a; $\varphi = \pi/2$ is, however, not mandatory). Then, the two-dimensional image detector is no longer needed since the image can be processed by a one-dimensional CCD array. This simplifies the image processing.

8.1. Experimental results on the SPS machine

In order to prove the principle, we used the industrial source which provides, without lenses

and collimators, a conical beam (instead of an ideal uniform cylindrical beam obtained by well-matched optics). The collector consists of an MCP followed by a luminescent screen which is observed by a camera. The image obtained every 40 ms from the camera is processed so as to obtain the ion-beam density. During the SPS acceleration ramp one can qualitatively observe the changes of the ion beam density, which is a consequence of the variation of the proton beam transverse dimension and position. The experimental measurements are shown in Figs. 6b–e.

These preliminary measurements are encouraging but still need accurate calibration. This

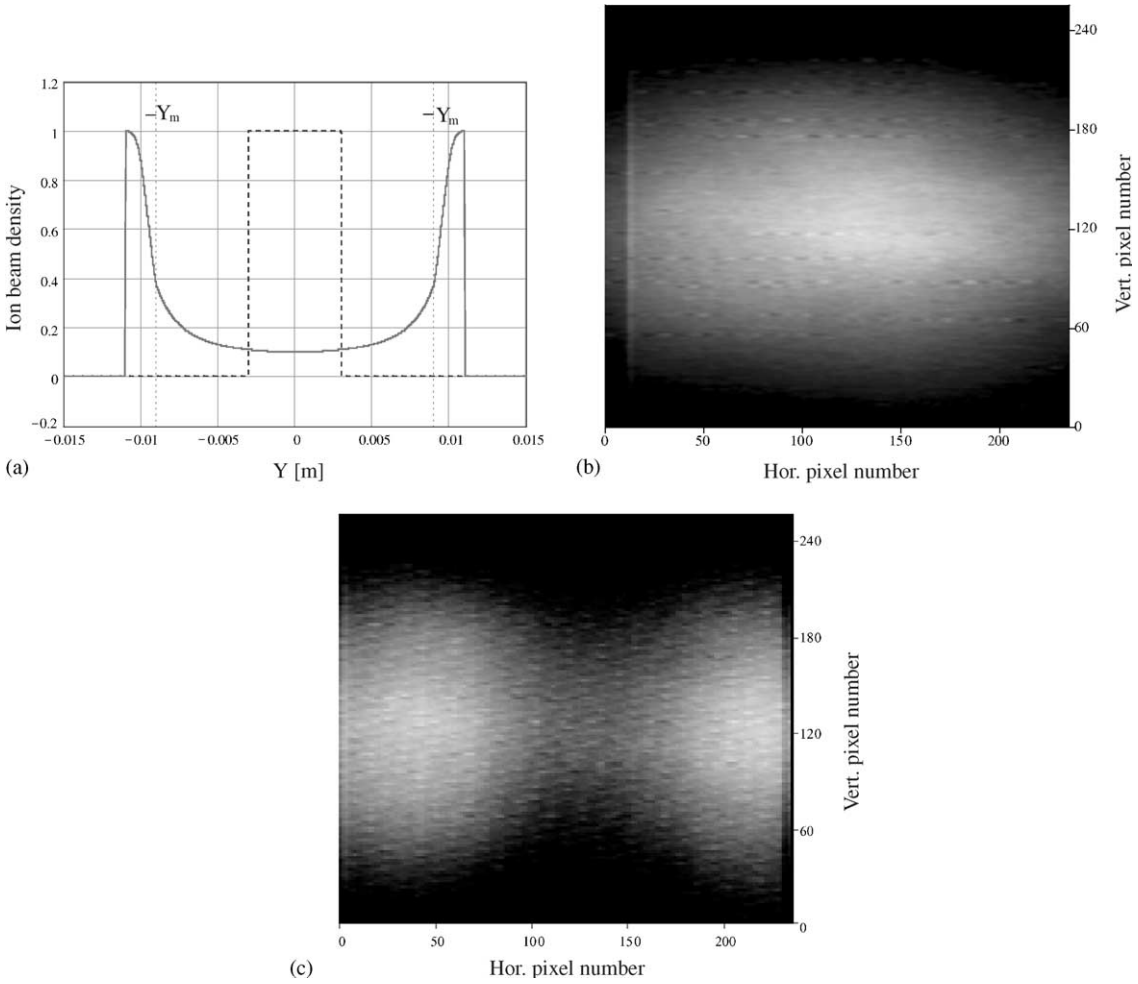

Fig. 6. Shadowing technique. Theoretical principle and experiments made on the SPS with 2.8×10^{13} circulating protons. We used Xe^{+} ions at 3.75 keV. (a) Theoretical computation. (Vertical axis: ion beam density, horizontal axis ordinate Y on the collector.) Proton beam OFF: dashed curve. Proton beam ON: solid curve, with $\Delta_r = 1$ mm, $\theta_{max} = 20$ mrad and $L = 0.4$ m; the vertical lines $\pm Y_m$ correspond to $Y_m = \Delta_r + L\theta_{max}$. Image observed on a TV screen when the proton beam is OFF (b), and when the proton beam is ON (c). (d) Depletion on horizontal ion densities observed on the luminescent screen at different instants of the SPS cycle (the number after AT represents milliseconds). Horizontal and vertical axis in arbitrary units. (e) Valley range distribution versus time. Vertical axis density in arbitrary units. Horizontal axis: position Y_0 on the collector (arbitrary units, i.e. number of pixels). Longitudinal axis: time in ms.

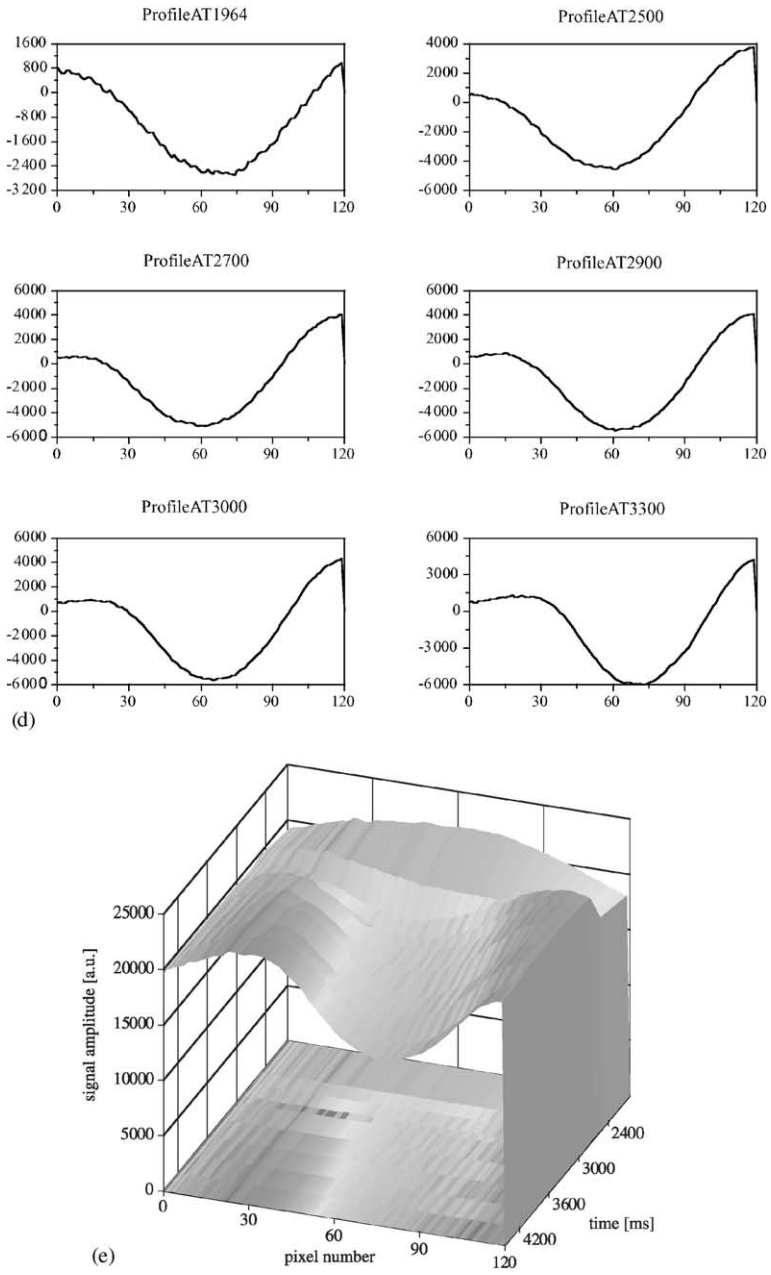

Fig. 6 (*continued*).

method, though involving a few difficulties in the exact determination of the proton-beam profile, acts as a quasi non-interceptive TV screen.

9. Use on the Linac

This type of detector can be used on other accelerators such as the Linac, Booster, or PS

where dense bunches are of interest. This is actually the case in the Linac where $n_b = 4.64 \times 10^9$ p/bunch.

The Linac 50 MeV proton bunch is non-relativistic and therefore the longitudinal electric field component has to be taken into account as well. In fact, the longitudinal field at the head of the bunch and that at the end of the bunch is opposite. Simulations [4] show that their effects almost cancel out so that a purely transverse electric field can in practice be considered. An exact analytical demonstration is out of the scope of this paper.

For our test we used the ion pencil-beam technique. As collector we used a resistive rectangular plate whose ends are connected to two low-pass amplifiers, A and B. The ion-beam centre of gravity is therefore given by

$$\langle Y(y_0)\rangle = \frac{A-B}{A+B}\ \text{constant}.$$

The present detector is not able to process a single bunch ($\sigma_t = 0.25$ ns). We thus limit our goal to the measurement of a full batch (duration of 50–100 μs) transverse profile. The pencil beam is therefore scanned through the beam in 50–100 μs. The principle of transverse profile measurement is shown in Fig. 7a. Experimental measurements are shown in Fig. 7b which can be compared with Fig. 7a. Since $y(t)$[m s^{-1}] is known, one can calibrate the transverse dimension versus time.

Keeping the pencil beam at a fixed position outside the batch, we measured its maximum deflection angle versus time; thus the intensity variation during the pulse (longitudinal profile of the batch) was determined and is shown in Fig. 7c.

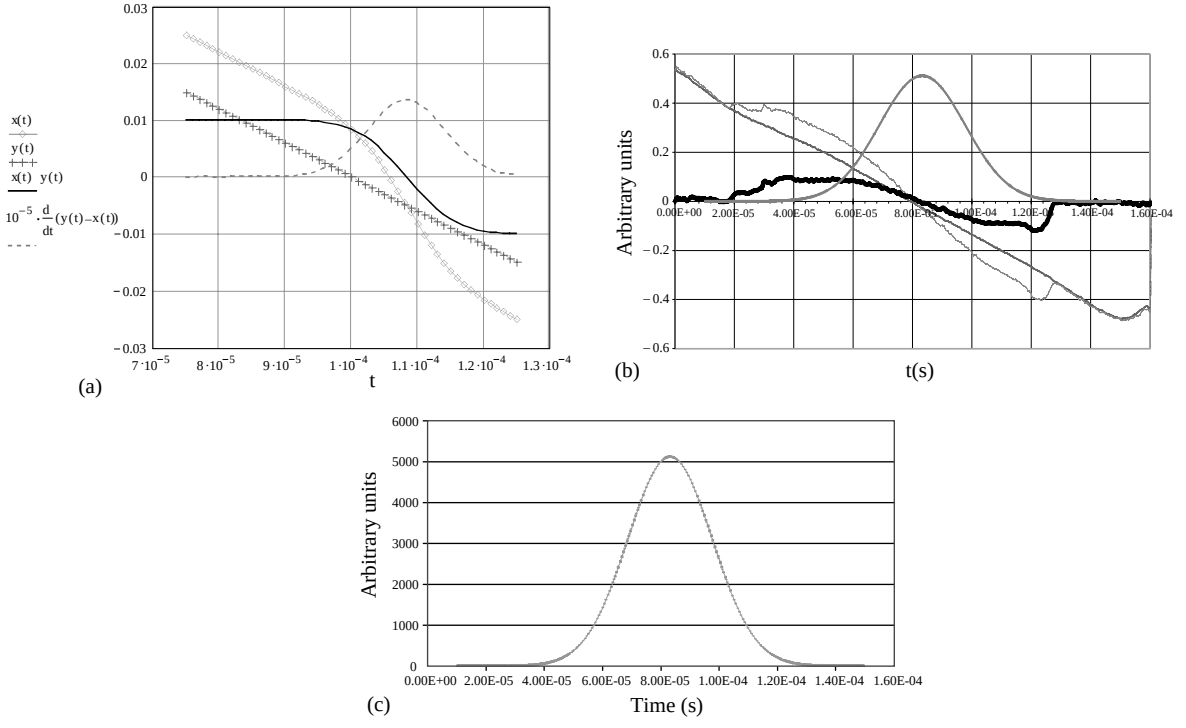

Fig. 7. Pencil-beam technique using a resistive plate as collector. (a) Calculations for a Gaussian proton beam. Horizontal axis t [s]. Vertical axis [arbitrary units]: (i) $y(t) = \langle Y(y_0)\rangle$ when the proton beam is OFF; (ii) $x(t) = \langle Y(y_0)\rangle$ when the proton beam is ON; (iii) $x(t) - y(t) = L\theta(t)$; (iv) the transverse proton-beam profile $\mathrm{d}(y(t) - x(t))/\mathrm{d}t$, multiplied by an arbitrary constant. (b) Measurement of the PS Linac batch. $x(t), y(t)$, $x(t) - y(t)$, can be compared to those of (a). The transverse batch profile obtained from the measurements (after an appropriate numerical fit) is also shown. (c) Measurement of the longitudinal batch profile.

10. Comments on accuracy and processing times

10.1. Accuracy

Let us define by σ_{er} the error introduced by the monitor on the actual beam r.m.s. dimension. The measured r.m.s. dimension is given by: $\sigma_m = \sqrt{\sigma^2 + \sigma_{er}^2}$, and the relative error by: $(\Delta\sigma/\sigma) = (\sigma_m - \sigma)/\sigma \cong 1/2(\sigma_{er}/\sigma)^2$. If for example we expect $\Delta\sigma/\sigma = \frac{1}{18}$ this would imply that $\sigma_{er} = \sigma/3$.

At the SPS where σ is of the order of 1 mm or more, a careful analysis of our measurements showed that:

- when using the pencil-beam technique with 1 mm width strip foils (spaced by 1.5 mm) (Section 6), we estimate $\sigma_{er} = 0.3$ mm and with a resistive plate (Section 9) $\sigma_{er} = 0.1$ mm;
- when using the curtain beam with a CCD camera (Section 7), we estimate $\sigma_{er} = 0.1$ mm (the accuracy being 1 pixel and the resolution 0.1 mm/pixel);
- in the future the use of strips spaced at 0.2 mm would reduce the error made on the r.m.s. dimension measurement to 0.1 mm. Concerning the use of image detectors, a conservative approach is to keep 0.1 mm/pixel. It must be kept in mind that the collector has to cope not only with the proton beam size but also with its displacement in time which reduces the r.m.s. measurement accuracy.

10.2. Processing time

With strips or resistive plates, the time interval between measured profiles is presently limited to 50 μs. Attempts are under way to reduce this time to 5 μs (it will also depend on the available source intensity). For light monitors, the standard processing time is presently 40 ms. Further reduction of this large time interval will depend on technological progress.

11. Conclusion

The proofs of principle of the three methods, namely the first using an ion pencil-beam, the second using a curtain beam, and the third making use of the shadowing technique, have been experimentally demonstrated. The ion source quality has to be improved as well as the electronic and processing techniques. With an improved detector, we can expect to measure profiles every 5 μs with an error on the r.m.s. dimension of the order of 50 μm for LHC-type beams. More details can be found in Ref. [8].

Acknowledgements

We want to thank G. Ferioli, G. Arduini and the SPS Vacuum team for their efficient help during our experiment. We also acknowledge the competence of the CERN Desktop Publishing Service in the drafting of this paper. Finally we thank the Mechanics Workshop of Lausanne University for their excellent work.

Appendix A

We aim to demonstrate that the deviation angle $\theta(y_0)$ can, under some assumptions, be approximated by an error function. We use the symbols already given in Section 2 and those shown in Fig. 1b.

A.1. Hypothesis

We consider a proton bunch having

- a transverse normalized distribution

$$n_\perp(r) = \frac{2}{2\pi\Delta_r^2}\exp\left(-\frac{r^2}{\Delta_r^2}\right), \quad r = \sqrt{x^2 + y^2}$$

  with r.m.s. value: $(\int_0^\infty r^2 n_\perp(r) 2\pi r\, dr)^{1/2} = \Delta_r$.
- a uniform longitudinal distribution over the length L_b so that the normalized longitudinal distribution $n_\sigma(z) = 1/L_b$.

So the overall distribution is

$$n(r) = n_b \frac{1}{L_b}\frac{2}{2\pi\Delta_r^2}\exp\left(-\frac{r^2}{\Delta_r^2}\right) \tag{A.1}$$

where $n_b \equiv$ number of protons/bunch.

A.2. Deflection angle as a function of the impact parameter y_0

It has been shown [1–3] that

$$\theta(y_0) = \frac{QV_0}{2E_k}\int_{-u_i}^{u_f} \frac{1-\exp[-y_0^2/\Delta_r^2(1+u^2)]}{1+u^2}\,du \tag{A.2}$$

$u \equiv x/y_0,\ u_f \equiv x_f/\Delta_r \gg 1,\ u_i \equiv x_i/\Delta_r \gg 1.$

Differentiating:

$$\frac{d\theta(y_0)}{dy_0} = \frac{QV_0}{2E_k}\frac{2y_0}{\Delta_r^2}\exp\left(-\frac{y_0^2}{\Delta_r^2}\right) \times \int_{-u_i}^{u_f} \exp\left[-\left(\frac{uy_0}{\Delta_r}\right)^2\right] du$$

and for $u_f, u_i \to \infty$ a good approximation will be

$$\left(\frac{d\theta(y_0)}{dy_0}\right)_{approx} = \frac{QV_0}{2E_k}\frac{2\sqrt{\pi}}{\Delta_r}\exp\left(-\frac{y_0^2}{\Delta_r^2}\right). \tag{A.3}$$

A.3. Error function

It is well known that

$$\mathrm{erf}(u) \equiv \frac{2}{\sqrt{\pi}}\int_0^u \exp(-\xi^2)\,d\xi,$$

$$\frac{d(\mathrm{erf}(u))}{du} = \frac{2}{\sqrt{\pi}}\exp(-u^2)$$

$\mathrm{erf}(0) = 0,\ \mathrm{erf}\ (\infty) = 1,\ \mathrm{erf}\ (x) = -\mathrm{erf}(-x).$

When applied to Eq. (A.3) this gives an approximate expression (A.4)

$$\theta_{approx}(y_0) = \frac{QV_0}{2E_k}\pi\ \mathrm{erf}\left(\frac{y_0}{\Delta_r}\right) + C \tag{A.4}$$

with the constant $C = 0$ since $\theta(0) = 0$.

We set the maximum deviation angle

$$\theta_{max} = \frac{QV_0}{2E_k}\pi \tag{A.5}$$

and are thus in position to summarize:

$$\theta_{approx}(y_0) = \theta_{max}\,\mathrm{erf}\left(\frac{y_0}{\Delta_r}\right) \tag{A.6}$$

$$\left(\frac{d\theta(y_0)}{dy_0}\right)_{approx} = \frac{2\theta_{max}}{\sqrt{\pi}\Delta_r}\exp\left(-\frac{y_0^2}{\Delta_r^2}\right) \tag{A.7}$$

$$\Delta_r = \frac{2\theta_{max}}{\sqrt{\pi}}\frac{1}{d\theta/dy_0|_{y_0\cong 0}}. \tag{A.8}$$

A.4. Another expression of the transverse r.m.s. value

Keeping the hypothesis of a Gaussian proton bunch:

- $n_\perp(r)$ is a two-dimensional Gaussian distribution ($r^2 = x^2 + y^2$) with r.m.s. value Δ_r.
- $(d\theta(y_0)/dy_0)_{approx}$ is a one-dimensional Gaussian distribution function of y_0 whose r.m.s. value is computed as follows:

$$\left[\frac{\int_{-\infty}^{\infty}(d\theta(y_0)/dy_0)_{approx}y_0^2\,dy_0}{\int_{-\infty}^{\infty}(d\theta(y_0)/dy_0)_{approx}\,dy_0}\right]^{1/2} = \frac{\Delta_r}{\sqrt{2}}.$$

It is convenient to set $\sigma \equiv \Delta_r/\sqrt{2}$ and to write instead

$$\theta_{approx}(y_0) = \theta_{max}\,\mathrm{erf}\left(\frac{y_0}{\sqrt{2}\sigma}\right) \tag{A.9}$$

$$\left(\frac{d\theta(y_0)}{dy_0}\right)_{approx} = 2\theta_{max}\frac{1}{\sqrt{2\pi}\sigma}\exp\left(-\frac{y_0^2}{2\sigma^2}\right) \tag{A.10}$$

$$\sigma = \frac{2\theta_{max}}{\sqrt{2\pi}}\frac{1}{d\theta/dy_0|_{y_0\cong 0}}. \tag{A.11}$$

Appendix B

We aim to analyse in more detail the theoretical aspects of the shadowing technique.

As already said, the ion distribution on the observer plane is expressed by

$$\frac{dn_i}{dY} = \frac{dn_i}{dy}\frac{dy}{dY} \tag{B.1}$$

where dn_i/dy is the ion distribution measured when the proton beam is OFF.

We have

$$Y = y + L\theta(y) \equiv g(y) \quad \text{or} \quad y = g^{-1}(Y).$$

From Eqs. (2a) and (2c):

$$\theta(y) = \theta_{\max} \operatorname{erf}\left(\frac{y}{\Delta_r}\right)$$

$$\frac{d\theta(y)}{dy} = \frac{2\theta_{\max}}{\sqrt{\pi}\Delta_r} \exp\left(-\frac{y^2}{\Delta_r^2}\right).$$

The function $g(y)$ itself is not simple and therefore g^{-1} is not straightforward.

Since

$$\frac{d(g^{-1}(Y))}{dY} = \frac{1}{dg/dy|_{y=g^{-1}(Y)}}$$

and

$$\frac{dg(y)}{dy} = 1 + L\frac{2\theta_{\max}(n_b)}{\sqrt{\pi}\Delta_r} \exp\left(-\frac{y^2}{\Delta_r^2}\right)$$

we obtain

$$\frac{d(g^{-1}(Y))}{dY} = \frac{dy}{dY}(Y) = \frac{1}{1 + L(2\theta_{\max}(n_b)/\sqrt{\pi}\Delta_r)\exp(-(g^{-1}(Y)/\Delta_r)^2)} \quad \text{(B.2)}$$

remembering that $\theta_{\max}$ depends on n_b and therefore on the proton beam intensity.

To illustrate this effect let us consider a simplified expression instead of an error function:

$$\theta(y) = \begin{cases} \theta_{\max}(n_b)\dfrac{y}{\Delta_r} & \text{for } |y| \leqslant 2\Delta_r \\ \theta_{\max}(n_b) & \text{for } |y| > 2\Delta_r \end{cases}$$

$$g(y) = Y(y) = \begin{cases} y + L\theta_{\max}(n_b)\dfrac{y}{\Delta_r} & \text{for } |y| \leqslant 2\Delta_r \\ y + L\theta_{\max}(n_b) & \text{for } |y| > 2\Delta_r \end{cases}$$

$$g^{-1}(Y) = y(Y) = \begin{cases} \dfrac{Y}{1 + L\theta_{\max}(n_b)/\Delta_r} & \text{for } |Y| \leqslant 2\Delta_r + L\theta_{\max}(n_b) \\ Y - L\theta_{\max}\ (n_b) & \text{for } |Y| > 2\Delta_r + L\theta_{\max}(n_b). \end{cases}$$

Then we have:

$$\frac{dn_i}{dY} = \frac{dn_i}{dy}\begin{cases} \dfrac{1}{1 + L\theta_{\max}(n_b)/\Delta_r} & \text{for } |Y| \leqslant 2\Delta_r + L\theta_{\max}(n_b) \\ 1 & \text{for } |Y| > 2\Delta_r + L\theta_{\max}(n_b). \end{cases}$$

Fig. 8 shows the curves dn_i/dY as a function of Y for $\Delta_r = 10^{-3}$ m, $L = 0.5$ m and for two different values of $\theta_{\max}$, namely for $\theta_{\max} = 5 \times 10^{-3}$ rad (curve dn_i1/dY on the plot) and for $\theta_{\max} = 10 \times 10^{-3}$ rad (curve dn_i2/dY on the plot). We considered only the simple case in which the initial ion curtain distribution is uniform, that is $(dn_i/dy) = \text{const} = 1$.

We see that the depletion width on the luminescent screen is $2(2\Delta_r + L\theta_{\max}(n_b))$.

The discontinuity of the curve occurs at $Y = (2\Delta_r + L\theta_{\max}(n_b))$ and will remain at this point if Δ_r and $\theta_{\max}$ both vary in such a way that $d(Y) = d\ (2\Delta_r + L\theta_{\max}(n_b)) = 0$, or $2d(\Delta_r) = Ld(\theta_{\max}(n_b))$, i.e. the r.m.s. proton beam size variation $d(\Delta_r)$ is compensated by a variation of $\theta_{\max}$ due to an increase of bunch intensity (n_b) and vice versa.

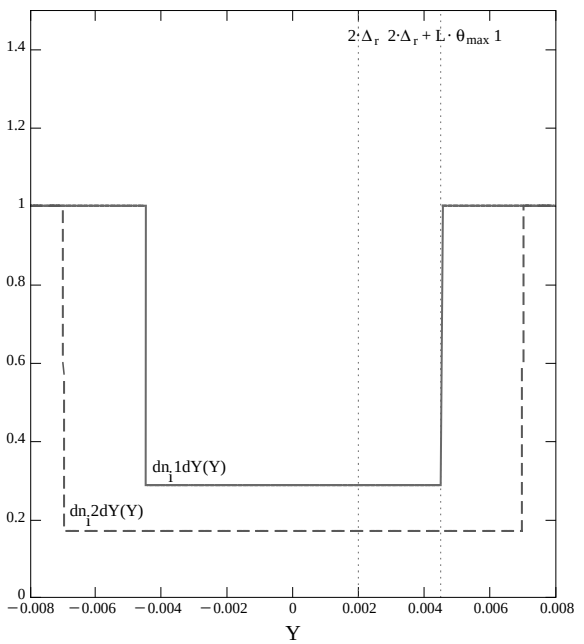

Fig. 8.

References

[1] J. Bosser, I. Meshkov, Profilometer for small dimension proton beam, CERN-PS/BD/Note 94-04, CERN, 7 March 1994.

[2] W. Nexsen, et al., Minimal interference beam size/profile measurement technique applicable to the collider, Superconducting Super Collider Laboratory, SSCL-631, May, 1993.

[3] E. Tsyganov, et al., Electron beam emittance monitor for the SSC, in: Proceedings of the 1993 Particle Accelerator Conference, Vol. 3, Washington, IEEE, Piscataway, NJ, 1994, pp. 2489–2491.

[4] J. Bosser, A. Feschenko, R. Maccaferri, Ion profilometer for the SPS and LHC accelerators, CERN-PS/BD/Note 99-07, CERN, September 1999.

[5] J.A. Pasour, Mai T. Ngo, Ion probe beam position and profile measurement, in: G.H. Mackenzie, B. Rawnsley, J. Thomson (Eds.), Proceedings of the Sixth Workshop on Beam Instrumentation, Vancouver, 1994, AIP Conference Proceedings No. 333, AIP, Woodbury, NY, 1995.

[6] J. Bosser, E. Chevallay, C. Dimopoulou, A. Feschenko, R. Maccaferri, Ion curtain profilometer, CERN-PS/BD/Note 99-15, CERN, 1999.

[7] C. Bovet (CERN), private communication.

[8] J. Bosser, C. Dimopoulou, A. Feschenko, R. Maccaferri, Transverse profile monitor using ion probe beams, CERN Internal Report PS/2000-071 (BD), November 2000.